An Interferometric Characterization Technique for Extreme Impedance Microwave Devices

Haris Votsi*, Laurence T. Stant*, Cristian Matei*, Martin J. Salter†, Chong Li‡, Nick M. Ridler†, Peter H. Aaen§

*Advanced Technology Institute, University of Surrey, Guildford, UK
†National Physical Laboratory, Teddington, UK
‡School of Engineering, University of Glasgow, Glasgow, UK
§Department of Electrical Engineering, Colorado School of Mines, Golden, Colorado, USA

***Abstract*—This paper presents a microwave impedance characterization technique for extreme impedance devices. The method is based on active interferometry and uses a 2-source 4-port vector network analyzer, which allows for a compact and straight-forward implementation. A new calibration algorithm is described that incorporates error terms from two separate three-known-load calibrations. Based on simulated and measured data, the proposed technique shows substantial improvement in obtaining the impedance of two offset-short devices when compared with conventional measurements.**

***Index Terms*—Calibration, extreme impedance measurement, interferometry, vector network analyzer.**

I. Introduction

NANOSCALE materials are being widely considered for future high-frequency applications as they have unique electrical and mechanical characteristics [1]. Such devices have very high impedance values, ranging from kΩ to MΩ. These impedances (Z_L) are considerably larger than the 50-Ω reference impedance (Z_0) of microwave frequency measuring instruments, such as vector network analyzers (VNAs). Their measurement results in very high reflection coefficients (Γ) as they reflect a large fraction of the incident electromagnetic (EM) energy as expressed by $\Gamma = (Z_L - Z_0)/(Z_L + Z_0)$. The variation of Γ based on the load impedance is plotted in Fig. 1, having lower sensitivity, $\partial\Gamma/\partial Z_L$, in the extreme impedance regions. Conventional microwave measurement methods and equipment lack the measurement sensitivity to characterize devices within these regions [2], [3]. For the accurate broadband characterization of extreme impedance devices the development of new metrology techniques is essential.

Several research groups have been working to mitigate this limitation. The majority of the publications are based on interferometry, relying on the minimization of the reflected wave by adding to it an opposite phase signal (cancellation wave) either reflected from a known impedance (passive) or generated from a controlled source (active). This results in a measurement with $\Gamma \approx 0$, where the VNA has the highest accuracy and low measurement noise. In [4]–[7] several passive measurement configurations have been proposed whereas in [8]–[12] active configurations were used.

This paper presents an interferometry-based method for the impedance characterization of extreme impedance microwave devices. Comparing to [12] a new calibration algorithm has been developed that translates the measurement reference plane to the device-under-test (DUT) and mitigates for the finite directivity of the directional coupler used for the combination of the reflected and cancellation waves. On-wafer measurements performed using the proposed method and using a conventional VNA are compared and discussed.

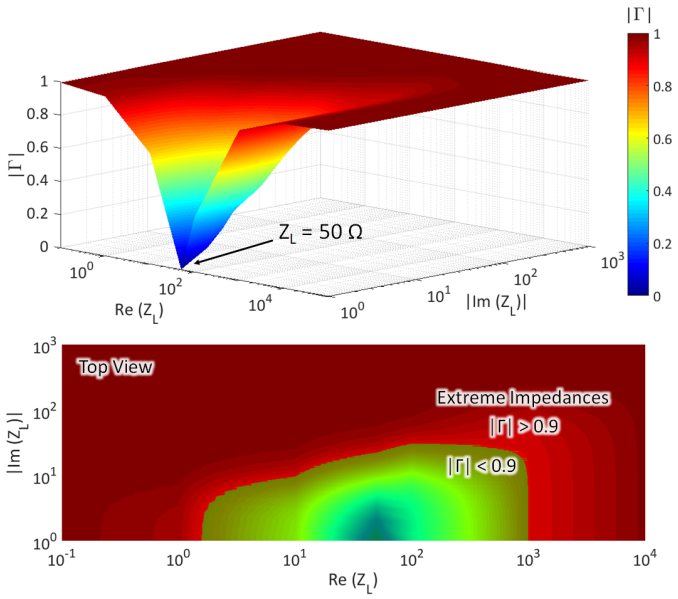

Fig. 1. Variation of reflection coefficient with the complex impedance. The region of extreme impedances at $|\Gamma| > 0.9$ is indicated.

II. Measurement Methodology

A. Theory

Fig. 2(a) shows the schematic diagram of the active interferometric method. The second source of the VNA is used to generate the cancellation wave and minimize the known reflection coefficient (Γ_{EIS}) of an extreme impedance standard (EIS). The amplitude and phase of the cancellation wave have to be set independently at each frequency. In this method, the cancellation wave is applied to the reflected wave of the EIS through a directional coupler. Provided the reflection coefficient of the EIS is known, then the same cancellation wave can be applied to other extreme impedance DUTs, as long as their reflection coefficients are close to Γ_{EIS}.

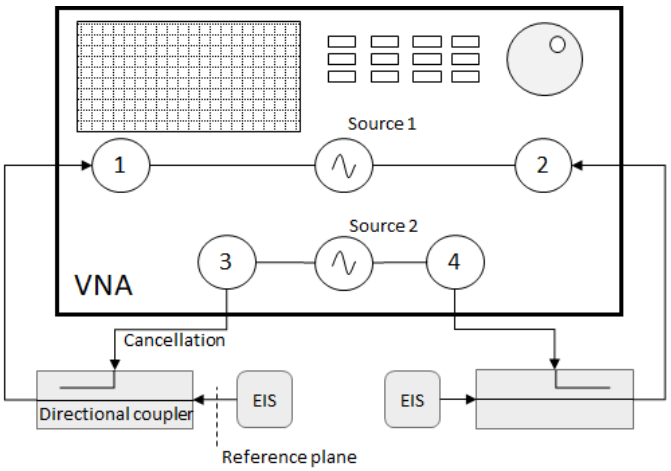

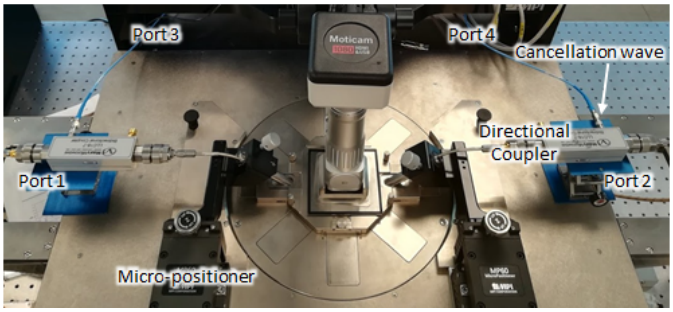

Fig. 2. Schematic and photograph of the measurement configuration of the active interferometric method.

Using the proposed method, the resultant reflection coefficients of the EIS and DUT with the cancellation wave on (Γ_{Eon} and Γ_{Don} respectively), and the known reflection coefficient of the EIS (Γ_{EIS}), are used to obtain the reflection coefficient (Γ_{method}) and the impedance (Z_{method}) of the DUT using (1) and (2) respectively. In this work, Γ_{Eon} is measured and can be accounted for in case of an imperfect cancellation. For comparison with conventional measurements, an extreme impedance DUT is also measured with the cancellation source turned off (Γ_{DUT}).

$$\Gamma_{method} = \Gamma_{Don} + \Gamma_{EIS} - \Gamma_{Eon} \tag{1}$$

$$Z_{method} = Z_0 \frac{1+\Gamma_{method}}{1-\Gamma_{method}} \tag{2}$$

B. Measurement Configuration

A 2-source 4-port Keysight N5247A 67 GHz PNA-X network analyzer was used for the measurements. The amplitude and phase of the second source of the VNA were controlled using the source phase control option available on the PNA-X (Option 088). Fig. 2 shows the schematic and photograph of the measurement configuration used. Source 1 of the PNA-X is used to provide the excitation signal to the DUT through Ports 1 and 2, whereas source 2 provides the cancellation wave through Ports 3 and 4. In this paper, Ports 1 and 3, and Ports 2 and 4 were paired to measure

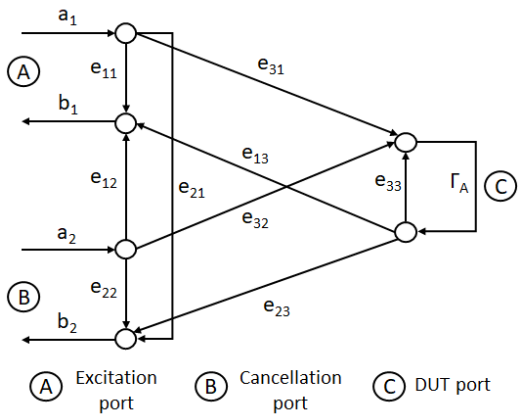

Fig. 3. Signal flow diagram for the measurement of the reflection coefficient using the proposed method.

the reflection coefficients of two 1-port extreme impedance DUTs. However, a similar configuration can be utilised for the impedance characterisation of 2-port devices using a suitable calibration algorithm.

C. Calibration Algorithm

A calibration algorithm has been developed to move the measurement reference plane to a 1-port DUT. Comparing with [12] the algorithm developed still relies on the measurement of three known standards, and it also mitigates for the finite directivity of the directional couplers used. A non-ideal directivity will result in a portion of the cancellation wave being coupled towards the DUT and being reflected towards the VNA port and this depends on the load impedance. This means that the same cancellation wave will perturb the measured reflection coefficient differently depending on different load impedances, so the finite directivity of the coupler must be accounted for in the calibration.

The calibration algorithm is based on measuring three known standards (Short-Open-Load in this case) under two different conditions; the cancellation wave turned on and off. The signal flow diagram, including the error terms of the method, for a 1-port measurement is shown in Fig. 3 [13]. Three ports are included within the diagram representing the excitation port (Port A), the cancellation port (Port B) and the DUT (Port C).

Equations (3) and (4) express the measured reflection coefficient (S_{11} in this case) under the conditions of the cancellation wave (a_2) being off and on respectively. The actual reflection coefficient of the DUT is expressed by Γ_A. All the error terms (e) in both conditions are collected within three calibration coefficients (E_1, E_2, E_3). The desired cancellation wave is represented by $\frac{a_2}{a_1}e_{12}$, whereas the unwanted contribution to the wave, which is Γ_A dependent, is expressed by $\frac{a_2}{a_1}(e_{32}e_{13} - e_{12}e_{33})\Gamma_A$, as shown in (4). To correct for this unwanted contribution, the algorithm used when the cancellation wave is on, is described by (5) and (6). To obtain the three calibration coefficients, (7) to (9) are used in both of

$$S_{11_{OFF}} = \frac{b_1}{a_1} = \frac{e_{11} + \Gamma_A(e_{31}e_{13} - e_{11}e_{33})}{1 - \Gamma_A e_{33}} = \frac{E_{1_{OFF}} + \Gamma_A E_{2_{OFF}}}{1 - \Gamma_A E_{3_{OFF}}} \tag{3}$$

$$S_{11_{ON}} = \frac{b_1}{a_1} = \frac{e_{11} + \frac{a_2}{a_1}e_{12} + \Gamma_A[e_{31}e_{13} - e_{11}e_{33} + \frac{a_2}{a_1}(e_{32}e_{13} - e_{12}e_{33})]}{1 - \Gamma_A e_{33}} = \frac{E_{1_{ON}} + \Gamma_A E_{2_{ON}}}{1 - \Gamma_A E_{3_{ON}}} \tag{4}$$

the calibrations with the cancellation wave turned on and off, where S and Γ represent the measured and actual reflection coefficients of the standard measured respectively. The first of the calibration coefficients ($E_{1_{OFF}}$) is obtained from the off calibration, the second ($E_{2_{ON}}$) from the on calibration in order to correct for the unwanted contribution to the cancellation wave, whereas the third calibration coefficient (E_3) can be obtained from either calibration, since it is the same.

$$S_{11_{method}} = \frac{E_{1_{OFF}} + \Gamma_A E_{2_{ON}}}{1 - \Gamma_A E_3} \tag{5}$$

$$\Gamma_{A_{method}} = \frac{S_{11_{method}} - E_{1_{OFF}}}{E_{2_{ON}} + S_{11_{method}} E_3} \tag{6}$$

$$E_3 = \frac{(S_2 - S_1)(\Gamma_3 + \Gamma_1) - (S_3 - S_1)(\Gamma_2 - \Gamma_1)}{(\Gamma_1 S_1 - \Gamma_3 S_3)(\Gamma_2 - \Gamma_1) - (\Gamma_1 S_1 - \Gamma_2 S_2)(\Gamma_3 + \Gamma_1)} \tag{7}$$

$$E_2 = \frac{E_3(\Gamma_1 S_1 - \Gamma_2 S_2) + S_2 - S_1}{\Gamma_2 - \Gamma_1} \tag{8}$$

$$E_1 = S_1(1 - E_3\Gamma_1) - E_2\Gamma_1 \tag{9}$$

A flow chart of the calibration procedure followed to obtain the reflection coefficients used in the method is shown in Fig. 4. The calibration algorithm is applied by post-processing the uncorrected measured data obtained by the VNA. The injected wave is applied at various power levels and phases to both the EIS and the DUT. Therefore, it is possible to investigate and find the optimum combination that minimizes the reflection coefficient of the EIS, and the measured data obtained at that specific combination are used subsequently to obtain the final results. The corrected Γ_{EIS} and Γ_{DUT} are obtained using the off calibration in order to be used in (1) and for comparison purposes respectively. This procedure is followed separately for both Ports 1 and 2 in combination with Ports 3 and 4 respectively.

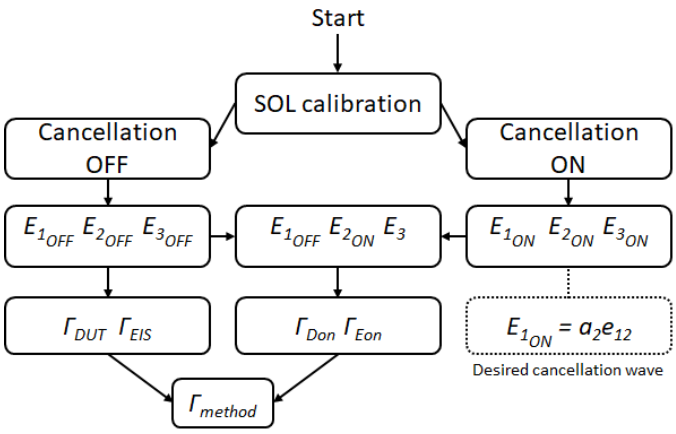

Fig. 4. Flow chart of the calibration procedure followed to extract the error terms used for the measurement of the reflection coefficients.

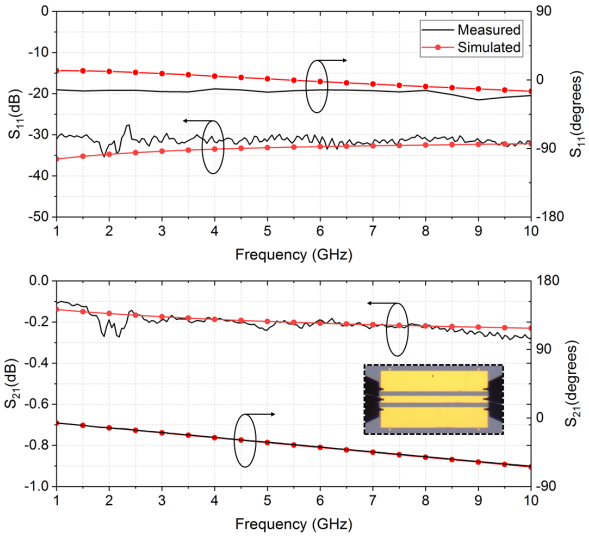

Fig. 5. Measured and simulated reflection and transmission coefficients transmission coefficient of a 50-Ω CPW line (inset).

III. Measurements & Results

A. Electromagnetic Simulations

For the validation of the method, the measured data using both the aforementioned technique and the conventional method have been compared with EM simulations of the DUTs. To ensure that the EM simulations accurately simulate the reflection coefficients of the DUTs, a 50-Ω 2-mm long coplanar-waveguide (CPW) line, located on the same wafer as the extreme impedance DUTs, was measured and simulated. Microscope measurements were performed to measure the dimensions of the gold line conductors, and these were included in the EM simulator (*em*™ from Sonnet Software). The width of the signal line of the CPW was measured to be 100 μm, separated by 66 μm from the two ground planes [14]. The conductivity of the conductors (3×10^8 S/m) and the dielectric constant (12.9) of the dielectric substrate (GaAs) were provided by the wafer manufacturer. Using SEM characterization the conductor thickness was measured to be 500 nm ±25 nm. The frequency range of the measurement and simulation was set to 1–10 GHz. A Short-Open-Load-Thru calibration was performed on an impedance standard substrate (ISS) to move

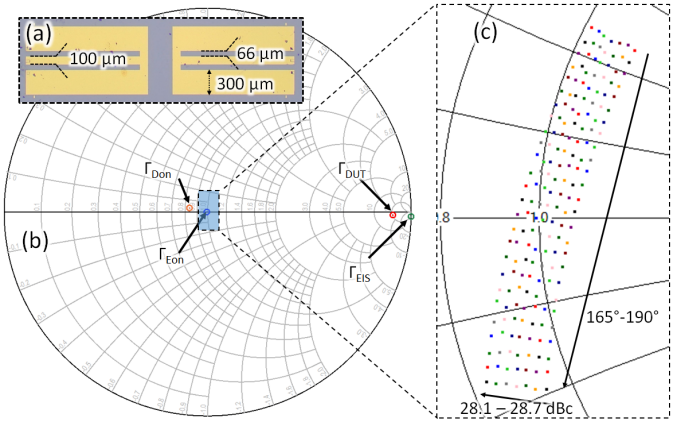

Fig. 6. (a) Offset shorts used as DUTs. (b) Smith chart including the post calibrated reflections coefficients using Ports 1 and 3. (c) Post-calibrated Γ_{Eon} measurements within a specific range of the cancellation wave. Each dot on the inset shows the resultant Γ_{Eon} under a specific cancellation wave. The Γ_{Eon} selected for this method is the one closest to the centre of the Smith chart (28.5 dBc / 179°).

TABLE I
GENERATED CANCELLATION WAVES

Port	Power (dBc)	Phase (°)	Selected Wave
3	27.3 – 30	165 – 190	28.5 dBc / 179°
4	27 – 29.5	240 – 270	28.2 dBc / 262°

the reference plane of the measurement to the ground-signal-ground (GSG) probe tips. Thru-Reflect-Line structures placed on the same wafer, were measured to remove the probe pads and obtain the S-parameters of the 50-Ω line only. Fig. 5 shows the measured and simulated reflection and transmission coefficients. The selected simulation parameters show a good agreement with the measured S-parameters of the line.

B. Devices & Specifications

The extreme impedance devices selected were two offset shorts. The devices are shown in Fig. 6(a). The two DUTs have the same width and gap dimensions as the 50-Ω CPW line described in Section III-A, and lengths of 3.3 mm. The shorted end of the line is 100 µm long. The frequency of the measurement was set to 8.39 GHz, as these offset shorts have an extremely high impedance at this frequency (≈1 kΩ). The input power at the two ports was set to -20 dBm and the intermediate frequency bandwidth (IFBW) at 10 Hz to increase the signal-to-noise ratio. The low-loss directional couplers used have an operational bandwidth between 1–18 GHz and a coupling factor of 30 dB.

For the measurements, two SOL calibrations were performed on both ports using an AC-2 on-wafer calibration substrate. Two open circuit standards located on the AC-2 substrate were used as the EISs for the proposed technique, as they have a reflection coefficient with similar phase to the DUTs' reflection at the desired frequency, and the cancellation wave will appropriately bring the combined reflection of the DUT close to zero. Furthermore all the required measurements

TABLE II
MEASURED AND SIMULATED REFLECTION COEFFICIENTS AND IMPEDANCES

Port	1	2
Γ_{DUT}	|0.9100| / -0.90°	|0.9111| / -1.12°
Γ_{method}	|0.9139| / -0.14°	|0.9116| / -0.53°
Γ_{EM}	|0.9136| / -0.11°	|0.9136| / -0.11°
Z_{DUT} (Ω)	1032 - j172	1029 - j217
Z_{method} (Ω)	1110 - j32	1070 - j107
Z_{EM} (Ω)	1107 - j24	1107 - j24

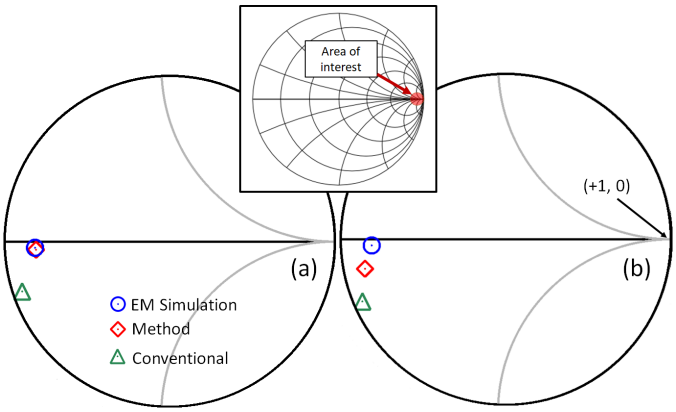

Fig. 7. Reflection coefficients, (a) S_{11} and (b) S_{22}, obtained through the active interferometric method, a conventional measurement and the EM simulation of the two offset shorts at 8.39 GHz.

of each device, with the cancellation wave on and off, were performed once the GSG probes had landed once, to avoid errors induced from the contact repeatability of the probe.

C. Measurement Data

For the cancellation of the EIS's reflection, the power and phase of the two cancellation ports (3 and 4) were varied between specific ranges before selecting the wave that minimised $|S_{11}|$ and $|S_{22}|$. The selected combination and ranges applied are shown in Table I. The cancellation port power was controlled in decibels relative to the input power (dBc). The step size for the power sweep was set to 0.1 dBc and for the phase sweep the step size was set to 1°. Fig. 6(c) illustrates the post-calibrated S_{11} of the EIS for a range of power and phase combinations applied as the cancellation wave, including the selected one (28.5 dBc / 179°). Each point on the Smith chart represents the resultant Γ_{Eon} under a specific cancellation wave.

The Smith chart presented in Fig. 6(b) includes the measured reflection coefficients of the EIS and DUT of Port 1, with the selected cancellation wave turned off and on. Fig. 7 shows the post-calibrated S_{11} and S_{22} of the offset shorts using the proposed active interferometric method (diamond) and a conventional measurement (triangle) at 8.39 GHz in the high impedance region of the Smith chart. The values of these reflections and the associated impedances are shown in Table II. At both ports the proposed method agrees closer

to the simulated impedance (Z_{EM}) of the devices when compared to the conventional measurements. The proposed method matches the simulation within 3+j8 Ω and 37+j83 Ω at Ports 1 and 2 respectively, whereas for the conventional measurement within 75+j148 Ω and 78+j193 Ω. The reduction in the percentage error in obtaining the DUTs' impedance, for either the real or the imaginary part, is 94% and 52% at Ports 1 and 2 respectively, when compared with the conventional measurements. The cancellation of the EIS's reflection coefficient was better at Port 1 ($|\Gamma_{Eon}|$ = 0.004) comparing with Port 2 ($|\Gamma_{Eon}|$ = 0.01). This explains the better agreement of the S_{11} measurement, as both Γ_{Eon} and Γ_{Don} were closer to 50 Ω.

IV. Conclusion

The initial steps towards developing an integrated extreme impedance measurement technique based on active interferometry, requiring only an external coupler have been presented. A new calibration algorithm based on two separate three-known-load calibrations, that mitigates for inaccuracies originating from the finite directivity of couplers used for the technique has been discussed. The method has been illustrated using a 2-source 4-port VNA and planar on-wafer DUTs. Simulated and measured data indicate that the proposed technique has successfully characterized the impedance of highly reflective devices, however, a rigorous uncertainty evaluation and comparison with other techniques is still required to fully justify the application of the method.

Acknowlegdement

This work was funded and supported by the Engineering and Physical Sciences Research Council (EPSRC) grant EP/L02263X/1. The authors wish to thank K. Haddadi, I. R. Jeune and G. Dambrine of the Institute of Electronics, Microelectronics and Nanotechnology, University of Lille, for the fabrication of the devices and the SEM characterization.

References

[1] T. M. Wallis, K. Kim, D. S. Filipovic, and P. Kabos, "Nanofibers for RF and beyond," *IEEE Microw. Magazine*, vol. 12, no. 7, pp. 51–61, Dec. 2011.

[2] H. Happy, K. Haddadi, D. Theron, T. Lasri, and G. Dambrine, "Measurement techniques for RF nanoelectronic devices: new equipment to overcome the problems of impedance and scale mismatch," *IEEE Microw. Mag.*, vol. 15, no. 1, pp. 30–39, Jan. 2014.

[3] T. M. Wallis and P. Kabos, *Measurement Techniques for Radio Frequency Nanoelectronics*. Cambridge University Press, 2017.

[4] M. Randus and K. Hoffmann, "A method for direct impedance measurement in microwave and millimeter-wave bands," *IEEE Trans. Microw. Theory Techn.*, vol. 59, no. 8, pp. 2123–2130, Aug. 2011.

[5] M. Randus and K. Hoffmann, "A simple method for extreme impedances measurement - experimental testing," in *Proc. 72nd ARFTG Microw. Meas. Conf.*, Portland, OR, 2008, pp. 40–44.

[6] A. Lewandowski, D. LeGolvan, R. A. Ginley, T. M. Wallis, A. Imtiaz, and P. Kabos, "Wideband measurement of extreme impedances with a multistate reflectometer," in *Proc. 72nd ARFTG Microw. Meas. Conf.*, Portland, OR, 2008, pp. 45–49.

[7] K. Haddadi and T. Lasri, "An interferometric technique for microwave measurement of high impedances," in *IEEE MTT-S Int. Microw. Symp. Dig.*, Montreal, QC, 2012, pp. 1–3.

[8] G. Vlachogiannakis, H. T. Shivamurthy, M. Pino, and M. Spirito, "An I/Q-mixer-steering interferometric technique for high-sensitivity measurement of extreme impedances," in *IEEE MTT-S Int. Microw. Symp. Dig.*, Phoenix, AZ, 2015, pp. 1–4.

[9] F. Mubarak, R. Romano, and M. Spirito, "Evaluation and modeling of measurement resolution of a vector network analyzer for extreme impedance measurements," in *Proc. 86th ARFTG Microw. Meas. Conf.*, Atlanta, GA, 2015, pp. 1–3.

[10] F. A. Mubarak, R. Romano, L. Galatro, V. Mascolo, G. Rietveld, and M. Spirito, "Noise behavior and implementation of interferometer-based broadband VNA," *IEEE Trans. Microw. Theory Techn.*, vol. 67, no. 1, pp. 249–260, Jan. 2019.

[11] R. Romano, F. Mubarak, M. Spirito, and L. Galatro, "The HΓ-VNA, an interferometric approach for the accurate measurement of extreme impedances," in *Proc. 93rd ARFTG Microw. Meas. Conf.*, Boston, MA, 2019, pp. 1–6.

[12] H. Votsi, C. Li, P. H. Aaen, and N. M. Ridler, "An active interferometric method for extreme impedance on-wafer device measurements," *IEEE Microw. Wireless Compon. Lett.*, vol. 27, no. 11, pp. 1034 – 1036, Sep. 2017.

[13] M. Randus and K. Hoffmann, "Microwave impedance measurement for nanoelectronics," *Radioengineering*, vol. 20, no. 1, pp. 276–283, Apr. 2011.

[14] H. Votsi, I. Roch-Jeune, K. Haddadi, C. Li, G. Dambrine, P. H. Aaen, and N. Ridler, "Development of a reference wafer for on-wafer testing of extreme impedance devices," in *Proc. 88th ARFTG Microw. Meas. Conf.*, Austin, TX, 2016, pp. 1–4.